Proceedings of the 2009 IEEE International Conference on Systems, Man, and Cybernetics
San Antonio, TX, USA - October 2009

# A Texture Energy Measurement Technique for 3D Volumetric Data

Motofumi T. Suzuki Yoshitomo Yaginuma Haruo Kodama
The Open University of Japan
CoDE, 2-11 Wakaba, Mihama-ku, Chiba-shi 261-8586, Japan
suzuki.motofumi@gmail.com, motofumi@code.u-air.ac.jp

***Abstract*—Recent advancements of 3D computer graphics hardware systems have made possible the handling of 3D volumetric data, and the amount of the available data has increased for various scientific fields. This paper proposes a pattern feature extraction method for 3D volumetric data. Pattern features are important for systems which require segmentation and classification. In this paper, the Laws texture energy approach is extended so that both 2D image data and 3D volumetric data can be handled. The Laws texture energy approach is a powerful technique for describing pattern features of 2D texture images, and it has been applied to various software applications. Our extension of the Laws texture energy approach enables direct extractions of pattern features from 3D volumetric data. Although the three dimensional extension increases the number of pattern features, the pattern features are reduced by combining similar pattern features. Our simulation software program attempts to reduce the number of shape features. The program rotates each feature along the $x$, $y$ and $z$ axes. The rotated features are evaluated if they are identical to other features, and the identical features are combined together to reduce the number of pattern features. For the experiments, artificially synthesized 3D solid textures are analyzed by using the 3D extended Laws features, and solid textures are classified by linear discriminant analysis (LDA). Our preliminary experiments show that the three dimensional extension of the Laws texture energy approach successfully classifies a certain database of 3D volumetric data.**

***Index Terms*—3D Volume Data, Voxel, Laws' Mask, Convolution, Solid Texture, Mask, Filter, Segmentation**

## I. Introduction

Recent advancements in computer graphics technology have made possible the visualization of 3D volumetric data. A large number of 3D volumetric data are available and are used for various scientific fields. It is very important that software systems can search and classify the volumetric data efficiently. Extractions of pattern features from volumetric data are important, because pattern features are used for indices of databases and are essential for classifications and segmentations.

Various approaches have been proposed for analyzing pattern features of 2D images [1] [2] [3] [4]. The approaches include edge frequency, run length encoding , wavelet, co-occurrence matrices , Fourier analysis , and autocorrelation . Recently, pattern feature extraction techniques for 3D volumetric data have been proposed which include extension of run-length encoding [5], GLCM (gray level co-occurrence matrices) [6] [7] [8] [9] and HLAC (Higher Order Local Autocorrelations) [10][11]. These originated from traditional 2D image analysis methods, but they are different in that they can handle 3D volumetric data. Although conversion of 3D volumetric data into multiple 2D images makes it possible to extract pattern features by traditional 2D image analysis methods, the conversion process is occasionally inefficient and sometimes results in loss of accuracy of pattern features. In contrast, these recently introduced 3D extended methods directly extract pattern features from 3D volumetric data without slicing into 2D images. In this research, we extend the Laws texture energy approach which is one of the efficient 2D texture analysis techniques. Our extension of the Laws texture energy approach enables extractions of pattern features from 3D volumetric data.

## II. Texture Energy Measures

This section describes (1) Laws' texture energy measures, (2) convolution computation, (3) combination of similar features and (4) linear discriminant analysis.

### A. Laws' Texture Energy Measures

The texture energy approach was proposed by K. I. Laws in 1979, and the approach has been used for various applications. Details of the approach can be found in many papers [12] [13]. The approach uses basic convolution kernels, and the kernels are applied to target 2D images.

Laws' one-dimensional convolution kernels of a length of three are as follows:

$$\begin{aligned} L3 &= (1, 2, 1) \\ E3 &= (-1, 0, 1) \\ S3 &= (-1, 2, -1) \end{aligned}$$

These labels stand for Level, Edge, and Spot. The lengths of the kernels can be extended by convolving the pairs of these kernels. For example, if these three kernels are convolved, five new kernels of a length of five are obtained:

$$\begin{aligned} L5 &= (1, 4, 6, 4, 1) \\ E5 &= (-1, -2, 0, 2, 1) \\ S5 &= (-1, 0, 2, 0, -1) \\ R5 &= (1, -4, 6, -4, 1) \\ W5 &= (-1, 2, 0, -2, 1) \end{aligned}$$

By extending the lengths of the kernels, new kernels referred to as Ripple and Wave are obtained. For analyzing

the 2D images, these sets of one-dimensional kernels are multiplied to obtain the two dimensional kernels. For the kernels of a length of three, there are 9 two dimensional kernels (3×3):

| | | |
|---|---|---|
| E3E3 | E3L3 | E3S3 |
| L3E3 | L3L3 | L3S3 |
| S3E3 | S3L3 | S3S3 |

From the kernels of a length of five, 25 two dimensional kernels (5×5) are obtained:

| | | | | |
|---|---|---|---|---|
| L5L5 | L5E5 | L5S5 | L5R5 | L5W5 |
| E5L5 | E5E5 | E5S5 | E5R5 | E5W5 |
| S5L5 | S5E5 | S5S5 | S5R5 | S5W5 |
| R5L5 | R5E5 | R5S5 | R5R5 | R5W5 |
| W5L5 | W5E5 | W5S5 | W5R5 | W5W5 |

All the kernels except for 'L3L3' and 'L5L5' are zero-sum kernels. These two special kernels are used for computing 'contrast' features of images, and are treated differently from other kernels.

| | | |
|---|---|---|
| E3E3E3 | E3E3L3 | E3E3S3 |
| E3L3E3 | E3L3L3 | E3L3S3 |
| E3S3E3 | E3S3L3 | E3S3S3 |
| L3E3E3 | L3E3L3 | L3E3S3 |
| L3L3E3 | L3L3L3 | L3L3S3 |
| L3S3E3 | L3S3L3 | L3S3S3 |
| S3E3E3 | S3E3L3 | S3E3S3 |
| S3L3E3 | S3L3L3 | S3L3S3 |
| S3S3E3 | S3S3L3 | S3S3S3 |

Fig. 1. Three dimensional Laws texture energy kernels (3×3×3).

For our experiments, 3D volumetric data are analyzed. Although the 3D volumetric data can be analyzed by using two dimensional kernels, these data have to be sliced into sequences of multiple 2D images. The slicing processes can require a considerable amount of time and can cause a loss of feature information. Therefore, in our experiments, two dimensional kernels are extended to three dimensional kernels. The use of the three dimensional kernels allows direct extraction of the shape features. The kernels of a length of three contain 27 (3×3×3) elements, and the kernels of a length of five contain 125 (5×5×5) elements as shown in Figures 1 and 2.

Most 2D image analysis applications for the Laws energy approach use kernels of lengths of three (3×3) and five (5×5). A kernel length can be stretched, for example, to 7×7, 9×9, 11×11 and so forth, when one-dimensional kernels are convolved repeatedly. The choice of appropriate lengths of kernels depends on applications and the target image to be analyzed. By changing the kernel sizes, pattern features extracted from images vary. For instance, small size kernels can better capture local area patterns compared to large size kernels. The use of large kernels allows the systems to capture coarse patterns from images.

| | | | |
|---|---|---|---|
| L5L5L5 | L5L5E5 | L5L5S5 | L5L5R5 |
| L5L5W5 | L5E5L5 | L5E5E5 | L5E5S5 |
| L5E5R5 | L5E5W5 | L5S5L5 | L5S5E5 |
| L5S5S5 | L5S5R5 | L5S5W5 | L5R5L5 |
| L5R5E5 | L5R5S5 | L5R5R5 | L5R5W5 |
| L5W5L5 | L5W5E5 | L5W5S5 | L5W5R5 |
| L5W5W5 | E5L5L5 | E5L5E5 | E5L5S5 |
| E5L5R5 | E5L5W5 | E5E5L5 | E5E5E5 |
| E5E5S5 | E5E5R5 | E5E5W5 | E5S5L5 |
| E5S5E5 | E5S5S5 | E5S5R5 | E5S5W5 |
| E5R5L5 | E5R5E5 | E5R5S5 | E5R5R5 |
| E5R5W5 | E5W5L5 | E5W5E5 | E5W5S5 |
| E5W5R5 | E5W5W5 | S5L5L5 | S5L5E5 |
| S5L5S5 | S5L5R5 | S5L5W5 | S5E5L5 |
| S5E5E5 | S5E5S5 | S5E5R5 | S5E5W5 |
| S5S5L5 | S5S5E5 | S5S5S5 | S5S5R5 |
| S5S5W5 | S5R5L5 | S5R5E5 | S5R5S5 |
| S5R5R5 | S5R5W5 | S5W5L5 | S5W5E5 |
| S5W5S5 | S5W5R5 | S5W5W5 | R5L5L5 |
| R5L5E5 | R5L5S5 | R5L5R5 | R5L5W5 |
| R5E5L5 | R5E5E5 | R5E5S5 | R5E5R5 |
| R5E5W5 | R5S5L5 | R5S5E5 | R5S5S5 |
| R5S5R5 | R5S5W5 | R5R5L5 | R5R5E5 |
| R5R5S5 | R5R5R5 | R5R5W5 | R5W5L5 |
| R5W5E5 | R5W5S5 | R5W5R5 | R5W5W5 |
| W5L5L5 | W5L5E5 | W5L5S5 | W5L5R5 |
| W5L5W5 | W5E5L5 | W5E5E5 | W5E5S5 |
| W5E5R5 | W5E5W5 | W5S5L5 | W5S5E5 |
| W5S5S5 | W5S5R5 | W5S5W5 | W5R5L5 |
| W5R5E5 | W5R5S5 | W5R5R5 | W5R5W5 |
| W5W5L5 | W5W5E5 | W5W5S5 | W5W5R5 |
| W5W5W5 | | | |

Fig. 2. Three dimensional Laws texture energy kernels (5×5×5).

*1) Convolution Computation:* Once the three dimensional kernels are obtained, these kernels can be used to scan across the 3D volumetric data. In the process, texture features of each voxel are computed. The final result of the process generates a set of new 3D volumetric data. The process can be expressed as the following equation (Equation 1).

$$g(x,y,z) = \sum_{i=\frac{-X}{2}}^{\frac{X}{2}} \sum_{j=\frac{-Y}{2}}^{\frac{Y}{2}} \sum_{k=\frac{-Z}{2}}^{\frac{Z}{2}} f(x-i, y-j, z-k)h(i,j,k) \quad (1)$$

where $f(x,y,z)$ is the volumetric data with a size of $X \times Y \times Z$, $g(x,y,z)$ is a result of convolved volumetric data, and $h(i,j,k)$ is a convolution kernel (filter).

Figure 3 shows an example of the input 3D volumetric data and the corresponding convolved 3D volumetric data. The image on the far left in the figure shows a slice of input volumetric data which contains two types of texture patterns. Other images are output images computed by the convolution process using the three dimensional Laws kernels of a length of three (3×3×3). Since there are 27 kernels, the same number of 27 volumetric data items is created. Although the actual output results show three dimensional volumetric data, the volumetric data are represented in sliced 2D images and only some portions of sliced images are shown because of space

limitation. As shown in the figure, some kernels are able to separate the data into two parts based on the texture patterns, and the border of the different patterns is separated by a plane. (In the case of 2D images, the patterns are separated by a border line rather than a plane.) In this example, the kernels 'L3S3L3' (white color border) and 'L3E3L3' (black color border) can separate the volumetric data into two parts based on texture patterns. This example shows how the three dimensional Laws kernels can be used for segmenting 3D volumetric data based on texture patterns.

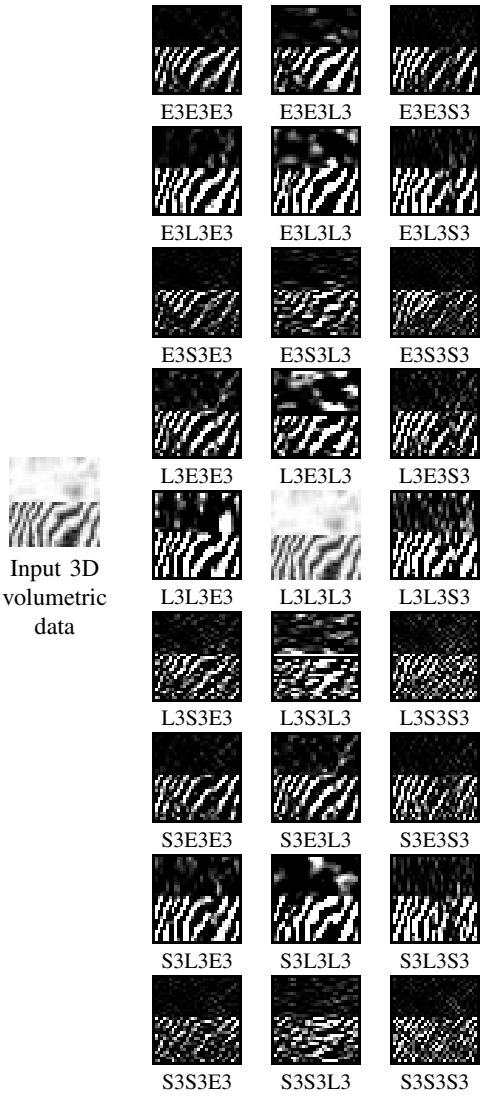


Fig. 3. A set of input 3D volumetric data (64×64×64) composed by two different texture patterns, and 27 sets of output data which are convolved by the three dimensional Laws kernels (3×3×3). The output volumetric data are represented in sliced 2D images.

### *B. Combination of Similar Features*

In the Laws energy approach [12] [13], similar features may be combined. For some texture analysis applications, directionality of texture patterns may be ignored. In the approach, kernels that contain identical elements are combined. For example, the kernels 'L3E3' and 'E3L3' are identical if one of the kernels is rotated in the order of 90 degrees. The kernel 'L3E3' can detect vertical patterns, and 'E3L3' can detect horizontal patterns. When both kernels are combined into one single kernel, the combined kernel can detect both vertical and horizontal patterns. The combined kernels are rotation invariant in the order of 90 degrees. In the case of the two dimensional kernel of a length of five, 25 kernels are reduced to 15 kernels. In the case of the two dimensional kernel of a length of three, 9 kernels are reduced to 6 kernels. The reduction for the number of kernels can help avoid the computation of high dimensional features, which improves pattern analysis results for certain applications.

The convolved images which are computed from combined kernels have to be properly weighted so that the entire features are normalized. For example, features of 'L3E3' and 'E3L3' are combined by 'addition,' and the combined features are divided by two. This single kernel can be notated by 'L3E3r', whereas 'r' means the kernel has a rotation invariant property. The computation is represented as Equation 2.

$$L3E3r = (L3E3 + E3L3) \times 0.5 \tag{2}$$

In the case of three dimensional kernels, a similar approach can be applied. For instance, rotations for one axis are considered for the two dimensional kernels, however, rotations for two axes are considered for three dimensional kernels. Since there are many elements for three dimensional kernels, detecting the combination of similar features is done by a simulation software program. The program rotates the three dimensional kernels along with the $x$, $y$ and $z$ axes, and looks for identical kernels which exist. If the kernels match at least the directions of two axes, they are combined together. For example, kernel 'L3L3E3' matches kernel 'E3L3L3' when rotated along the $y$ and $z$ axes, however, kernel 'L3L3E3' matches kernel L3E3L3' when rotated along the $x$ axis only. In these cases, kernels 'L3L3E3' and 'E3L3L3' are combined while kernels 'L3L3E3' and 'L3E3L3' are not. Figures 4 and 5 show the simulation program results for a list of the combined kernels. In the combination processes, the kernels of a length of three (3×3×3) are reduced to 18 from 27, and the kernels of a length of five (5×5×5) are reduced to 80 from 125.

By using the three dimensional Laws kernels for the convolution computations, pattern features of 3D volumetric data can be extracted. Once the pattern features are extracted, the features can be analyzed as to how they are related to texture patterns by using a statistical technique such as linear discriminant analysis (LDA).

### *C. Linear Discriminant Analysis*

In our experiments, a database of 3D solid textures is classified based on their pattern features. For the classifications,

| | | | |
|---|---|---|---|
| L3L3L3 | L3L3E3r | L3L3S3r | L3E3L3 |
| L3E3E3r | L3E3S3r | L3S3L3 | L3S3E3r |
| L3S3S3r | E3L3E3 | E3L3S3r | E3E3E3 |
| E3E3S3r | E3S3E3 | E3S3S3r | S3L3S3 |
| S3E3S3 | S3S3S3 | | |

Fig. 4. Combined kernels (3×3×3). Kernels are reduced to 18 from 27.

| | | | |
|---|---|---|---|
| L5L5L5 | L5L5E5r | L5L5S5r | L5L5R5r |
| L5L5W5r | L5E5L5 | L5E5E5r | L5E5S5r |
| L5E5R5r | L5E5W5r | L5S5L5 | L5S5E5r |
| L5S5S5r | L5S5R5r | L5S5W5r | L5R5L5 |
| L5R5E5r | L5R5S5r | L5R5R5r | L5R5W5r |
| L5W5L5 | L5W5E5r | L5W5S5r | L5W5R5r |
| L5W5W5r | E5L5E5 | E5L5S5r | E5L5R5r |
| E5L5W5 | E5E5E5 | E5E5S5r | E5E5R5r |
| E5E5W5 | E5S5E5 | E5S5S5r | E5S5R5r |
| E5S5W5 | E5R5E5 | E5R5S5r | E5R5R5r |
| E5R5W5 | E5W5E5 | E5W5S5r | E5W5R5r |
| E5W5W5 | S5L5S5 | S5L5R5r | S5L5W5r |
| S5E5S5 | S5E5R5r | S5E5W5r | S5S5S5 |
| S5S5R5r | S5S5W5r | S5R5S5 | S5R5R5r |
| S5R5W5r | S5W5S5 | S5W5R5r | S5W5W5r |
| R5L5R5 | R5L5W5r | R5E5R5 | R5E5W5r |
| R5S5R5 | R5S5W5r | R5R5R5 | R5R5W5r |
| R5W5R5 | R5W5W5r | W5L5E5 | W5L5W5 |
| W5E5E5 | W5E5W5 | W5S5E5 | W5S5W5 |
| W5R5E5 | W5R5W5 | W5W5E5 | W5W5W5 |

Fig. 5. Combined kernels (5×5×5). Kernels are reduced to 80 from 125.

Linear Discriminant Analysis (LDA) is applied to the pattern features. LDA is a popular statistical technique for classifying objects into groups based on a set of the objects' features or patterns. The analysis finds the best linear combination of features to separate the groups. Figure 6 shows a table of pattern features and texture categories , and these variables are analyzed by LDA.

## III. Experiments and Results

This section describes (1) experimental data, (2) statistical learning for texture classifications, (3) discriminant functions and (4) classification results.

### A. Experimental data

A 3D volumetric data synthesis program was implemented for the experiments. The program synthesizes 3D solid textures. For the creation of realistic textures [16] [14] [17] [18], stochastic functions were applied to the program. These functions are referred to as noise and return random values, which are important for the texture synthesis with natural patterns. We used the Perlin's noise function [15] which is one of

| Categories | features | | | | |
|---|---|---|---|---|---|
| cloud | $xc_{00}$ | $xc_{10}$ | $xc_{20}$ | $\cdots$ | $xc_{m0}$ |
| ⋮ | ⋮ | ⋮ | ⋮ | | ⋮ |
| cloud | $xc_{0n}$ | $xc_{1n}$ | $xc_{2n}$ | $\cdots$ | $xc_{mn}$ |
| marble | $xm_{00}$ | $xm_{10}$ | $xm_{20}$ | $\cdots$ | $xm_{m0}$ |
| ⋮ | ⋮ | ⋮ | ⋮ | | ⋮ |
| marble | $xm_{0n}$ | $xm_{1n}$ | $xm_{2n}$ | $\cdots$ | $xm_{mn}$ |
| turb. | $xt_{00}$ | $xt_{10}$ | $xt_{20}$ | $\cdots$ | $xt_{m0}$ |
| ⋮ | ⋮ | ⋮ | ⋮ | | ⋮ |
| turb. | $xt_{0n}$ | $xt_{1n}$ | $xt_{2n}$ | $\cdots$ | $xt_{mn}$ |
| wood | $xw_{00}$ | $xw_{10}$ | $xw_{20}$ | $\cdots$ | $xw_{m0}$ |
| ⋮ | ⋮ | ⋮ | ⋮ | | ⋮ |
| wood | $xw_{0n}$ | $xw_{1n}$ | $xw_{2n}$ | $\cdots$ | $xw_{mn}$ |

Fig. 6. A table of pattern features and texture categories. These variables are analyzed by LDA.

the important noise functions to synthesize 3D solid textures. Figure 7 shows four types of 3D solid textures synthesized by our experimental program. Each 3D solid texture has a size of 64×64×64. In Figure 7, the 2D slice of each 3D solid texture is also shown. In the experiments, a database of 3D solid textures is synthesized, and it contains a total of 200 textures (50 cloud, 50 marble, 50 turbulence and 50 wood). The texture for a training data set is chosen from the database. One hundred textures are selected randomly for training, and the other 100 are for testing. Each 3D solid texture has a size of 64×64×64, and it took about 10 hours to synthesize 200 textures by using a standard PC (Intel Pentium 4 processor running at 3.4GHz).

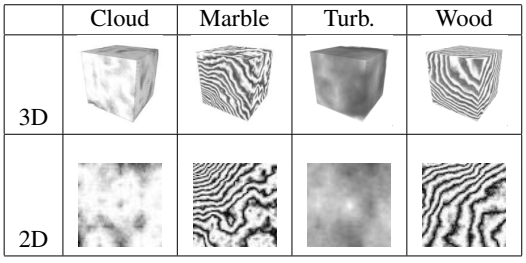


Fig. 7. Four types of solid textures (Cloud, Marble, Turbulence and Wood). Each 3D solid texture has a size of 64×64×64. The 2D slice of each 3D solid texture is also shown.

### B. Statistical Learning for Texture Classification

For LDA, if there are $G$ groups then it is possible to find $G-1$ linear discriminant functions which separate the groups. In our experimental case, since there are four categories of textures, three linear discriminant functions are used for texture classifications.

Figure 8 shows texture data (3×3×3 kernels) on discriminant coordinates, and Figure 9 shows texture data (5×5×5 kernels) on discriminant coordinates. Three discriminant functions are labeled $LD1$, $LD2$ and $LD3$. The labels 'C', 'M', 'T' and 'W' in the figure indicate types of textures. From

the figures, the 5×5×5 case has better separation observed between the four groups 'C', 'M', 'T' and 'W'. In the 3×3×3 case, several overlaps are observed between groups 'M' and 'W', which means there are some difficulties for discriminating between 'Marble' and 'Wood' textures when 3×3×3 kernels are used for these experiments.

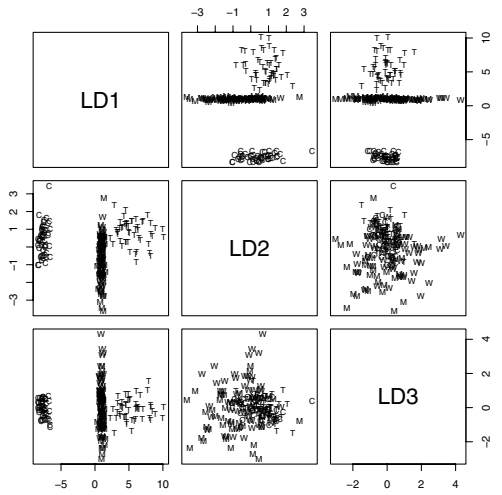


Fig. 8. Texture data on discriminant coordinates (3×3×3 kernels). Three discriminant functions are labeled LD1, LD2 and LD3. The labels 'C', 'M', 'T' and 'W' in the figure indicate types of textures. Several overlaps are observed between groups 'M' and 'W'.

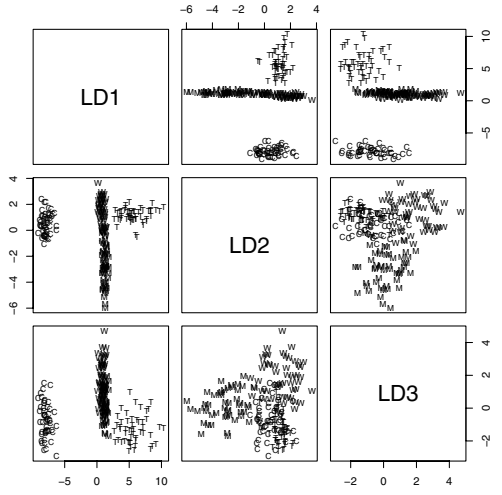


Fig. 9. Texture data on discriminant coordinates (5×5×5 kernels). Three discriminant functions are labeled LD1, LD2 and LD3. The labels 'C', 'M', 'T' and 'W' in the figure indicate types of textures.

### C. Discriminant Functions

In this experiment, the coefficients of discriminant functions are normalized before the analysis. In such a case, the coefficients of the predictors can be used for checking which predictors play an important role. For example, the larger the coefficient of a predictor of a discriminant function is, the more important role it plays. Figures 10 and 11 show coefficients of discriminant functions. In both figures, the top 3 influential coefficients for each function are marked by a box.

| Kernel | LD1 | LD2 | LD3 |
|---|---|---|---|
| L3L3L3 | -5.5751e-6 | -1.6307e-6 | -3.6911e-8 |
| L3L3E3r | 1.0820e-4 | 2.5810e-5 | -6.3937e-7 |
| L3L3S3r | 7.7020e-4 | 3.7896e-3 | -9.0460e-4 |
| L3E3L3 | 2.6813e-5 | -5.0123e-5 | -7.0396e-6 |
| L3E3E3r | -3.7220e-4 | -8.6472e-4 | 3.9345e-3 |
| L3E3S3r | 1.6282e-3 | 2.7489e-3 | -2.6400e-2 |
| L3S3L3 | 5.4657e-5 | 1.5080e-3 | 2.3246e-4 |
| L3S3E3r | -8.5172e-5 | 6.6375e-3 | -1.2570e-2 |
| L3S3S3r | -1.9470e-3 | -5.4264e-2 | -1.8391e-2 |
| E3L3E3 | 1.2532e-3 | 5.6275e-4 | -9.8635e-4 |
| E3L3S3r | -2.3214e-3 | 9.9135e-3 | 2.3392e-2 |
| E3E3E3 | -5.6546e-3 | 5.7450e-2 | 1.0377e-1 |
| E3E3S3r | 1.8600e-2 | -9.6467e-2 | -1.3165e-1 |
| E3S3E3 | -2.1006e-2 | 2.4550e-2 | 9.0034e-2 |
| E3S3S3r | -2.5208e-3 | 4.7784e-1 | 2.8958e-1 |
| S3L3S3 | -8.4180e-4 | -3.2878e-2 | 2.7080e-2 |
| S3E3S3 | 1.3393e-2 | -2.5701e-1 | -1.7507e-1 |
| S3S3S3 | 4.9885e-2 | 2.4208e-1 | -2.8495e-1 |

Fig. 10. Coefficients of discriminant functions (Kernel 3×3×3)

In the analysis, the eigenvalues can be computed for each discriminant function. These values reflect the amount of variance explained in the grouping variable by the predictors. Figure 12 shows the ratio of the eigenvalues to estimate the relative importance of discriminant functions. In our experiment, discriminant functions $LD1$ and $LD2$ have more discriminating power for both 3×3×3 and 5×5×5 cases.

| | LD1 | LD2 | LD3 |
|---|---|---|---|
| 3×3×3 | 0.9633 | 0.0314 | 0.0053 |
| 5×5×5 | 0.5403 | 0.3145 | 0.1452 |

Fig. 12. Proportions of eigenvalues for discriminant functions.

### D. Classification Results

Figure 13 shows how a set of test texture data is classified by the discriminant functions which are trained by the training data set. In the figure, rows represent predicted texture types, and columns represent actual texture types. A database of 3D solid textures which mentioned in section 3.1 is examined by using both 3×3×3 kernels and 5×5×5 kernels. There are 19 textures misclassified for the 3×3×3 case as shown in Figure 13. Thirty six percent (9/25) of 'Marble' textures are

| Kernel | LD1 | LD2 | LD3 | Kernel | LD1 | LD2 | LD3 |
|---|---|---|---|---|---|---|---|
| L5L5L5 | -2.1985e-8 | -1.3799e-7 | 3.5223e-8 | L5L5E5r | -9.4368e-7 | 1.5395e-6 | -2.3785e-6 |
| L5L5S5r | -1.8308e-6 | 8.6156e-5 | 2.0813e-5 | L5L5R5r | 8.1520e-4 | 1.3760e-4 | -2.4649e-4 |
| L5L5W5r | -7.5413e-4 | -3.5498e-4 | -7.7391e-4 | L5E5L5 | 1.1134e-6 | -4.8067e-7 | -6.3565e-7 |
| L5E5E5r | 1.0718e-4 | -9.7043e-5 | 5.9580e-5 | L5E5S5r | -3.6866e-3 | 1.0969e-3 | 9.2422e-5 |
| L5E5R5r | -5.6838e-3 | 2.8091e-4 | 9.6834e-3 | L5E5W5r | 9.7665e-3 | -8.9527e-3 | -2.3582e-3 |
| L5S5L5 | -1.2360e-5 | 2.3419e-5 | 1.4250e-5 | L5S5E5r | -7.9898e-4 | -7.3161e-4 | -2.0656e-3 |
| L5S5S5r | 1.2513e-2 | 6.9376e-3 | 2.0730e-3 | L5S5R5r | -9.2103e-3 | 8.6030e-3 | -1.9626e-2 |
| L5S5W5r | 2.5871e-2 | -3.0833e-2 | -1.1286e-2 | L5R5L5 | -1.8986e-4 | 8.5179e-5 | 2.2344e-4 |
| L5R5E5r | -6.4493e-3 | 3.5876e-3 | -5.2364e-3 | L5R5S5r | 1.3943e-2 | -1.8250e-2 | -1.5138e-2 |
| L5R5R5r | -2.0779e-4 | 5.6776e-3 | 9.5178e-3 | L5R5W5r | -6.0488e-3 | 1.7550e-2 | -1.3801e-2 |
| L5W5L5 | 3.4864e-4 | -3.4889e-5 | 1.0157e-4 | L5W5E5r | -1.6357e-3 | 5.5779e-3 | -4.2636e-3 |
| L5W5S5r | -1.4624e-2 | -6.1380e-3 | -1.9672e-3 | L5W5R5r | 3.0230e-2 | -1.3936e-2 | 3.0739e-2 |
| L5W5W5r | 5.6894e-3 | 8.5709e-3 | -1.5706e-2 | E5L5E5 | 1.9630e-5 | 6.5372e-5 | 8.7073e-6 |
| E5L5S5r | -3.5759e-4 | -1.1275e-3 | -5.3836e-4 | E5L5R5r | -7.8779e-3 | 5.2185e-3 | 4.4154e-3 |
| E5L5W5 | -5.8225e-3 | 5.2641e-3 | 3.3790e-3 | E5E5E5 | 8.9784e-4 | -9.7625e-4 | 2.1821e-3 |
| E5E5S5r | -7.0266e-2 | 4.0767e-2 | -3.0965e-2 | E5E5R5r | -1.6422e-1 | 3.0228e-2 | -3.7344e-2 |
| E5E5W5 | 2.2869e-1 | 1.0641e-3 | 6.6905e-2 | E5S5E5 | -4.0061e-2 | 9.3374e-3 | -2.6535e-2 |
| E5S5S5r | -7.2514e-1 | 3.3431e-1 | -1.0142e-1 | E5S5R5r | -1.6477e-1 | 1.4303e-1 | 1.5599e-1 |
| E5S5W5 | -2.1342e-1 | 7.3494e-2 | -3.0336e-1 | E5R5E5 | -4.4007e-2 | 4.1317e-2 | -1.0072e-2 |
| E5R5S5r | 5.0609e-1 | -1.2204e-1 | 1.6899e-1 | E5R5R5r | 9.4723e-2 | -8.0040e-2 | -4.8759e-2 |
| E5R5W5 | 1.3296e-1 | 4.0874e-2 | -1.6459e-1 | E5W5E5 | 5.3381e-3 | -3.3256e-2 | -3.9015e-2 |
| E5W5S5r | -7.2937e-1 | 3.8486e-2 | -3.4415e-1 | E5W5R5r | 2.7354e-1 | 3.3673e-1 | 1.4752e-1 |
| E5W5W5 | 7.6959e-1 | -2.1540e-1 | -3.4238e-1 | S5L5S5 | 2.1216e-2 | -6.5030e-3 | 8.2042e-3 |
| S5L5R5r | -6.4432e-3 | 5.7271e-6 | 9.7582e-3 | S5L5W5r | 3.3916e-2 | -1.2350e-3 | 3.4359e-2 |
| S5E5S5 | 7.8777e-2 | -7.9790e-2 | 4.5442e-2 | S5E5R5r | 4.4355e-1 | -8.5547e-2 | 1.6908e-1 |
| S5E5W5r | -7.0381e-1 | 5.4953e-1 | -5.1056e-1 | S5S5S5 | 1.277759 | 7.5831e-2 | 1.150618 |
| S5S5R5r | -2.614053 | -5.6713e-2 | -9.8777e-1 | S5S5W5r | -1.280188 | 8.9978e-1 | 5.2720e-2 |
| S5R5S5 | -2.3465e-1 | 1.1009e-1 | -3.5185e-1 | S5R5R5r | 6.0723e-1 | -3.5277e-1 | 4.9137e-2 |
| S5R5W5r | 9.6066e-1 | -4.9713e-1 | -2.1896e-2 | S5W5S5 | 1.194720 | -7.9601e-2 | 4.0133e-1 |
| S5W5R5r | -1.377659 | 1.1349e-1 | 1.8229e-1 | S5W5W5r | -2.622263 | -8.1807e-1 | -2.158224 |
| R5L5R5 | -9.1136e-3 | 2.8323e-3 | -7.4267e-3 | R5L5W5r | -3.7951e-2 | -1.5134e-2 | -1.2560e-2 |
| R5E5R5 | -3.0764e-1 | 8.2647e-2 | 3.0465e-2 | R5E5W5r | 2.9539e-2 | 2.6600e-1 | 1.1096e-1 |
| R5S5R5 | 4.8630e-1 | 1.7272e-2 | -1.9762e-1 | R5S5W5r | -1.9386e-1 | 9.5823e-1 | -1.4662e-2 |
| R5R5R5 | -2.5731e-1 | -6.1084e-3 | 1.8959e-2 | R5R5W5r | 9.0572e-1 | -2.0080e-1 | 8.0955e-1 |
| R5W5R5 | -8.4387e-2 | -1.2882e-1 | -2.7541e-2 | R5W5W5r | 1.587359 | 8.7106e-2 | 1.1053e-1 |
| W5L5E5 | 5.1573e-4 | -1.3721e-3 | 5.5985e-3 | W5L5W5 | -3.9266e-2 | 2.3354e-2 | 1.6825e-2 |
| W5E5E5 | -1.4806e-2 | 6.6912e-2 | 1.9041e-2 | W5E5W5 | 3.6158e-1 | 2.5440e-1 | 4.4309e-1 |
| W5S5E5 | -1.6438e-1 | -3.8398e-2 | 5.2633e-2 | W5S5W5 | -1.788010 | 1.268289 | -3.1313e-1 |
| W5R5E5 | -1.6777e-1 | 2.9319e-2 | -1.4372e-1 | W5R5W5 | -4.2104e-1 | 2.4430e-2 | -1.205343 |
| W5W5E5 | 1.9595e-1 | -1.4422e-1 | -3.0602e-1 | W5W5W5 | 2.162967 | 2.2851e-1 | 7.3831e-1 |

Fig. 11. Coefficients of discriminant functions (Kernel 5×5×5; 80 Pattern Features). The top 3 influential coefficients for each function are marked by boxes.

misclassified as 'Wood' textures, 4% (1/25) of 'Turbulence' textures are misclassified as 'Marble', and 36% (9/25) of 'Wood' textures are misclassified as 'Marble.' Therefore, 81% (81 out of 100) of test textures are classified correctly for the 3×3×3 kernels. As shown in Figure 13, 100% (100 out of 100) of test textures are classified correctly for the 5×5×5 kernels. In our preliminary experimental cases, the 5×5×5 kernels classify 3D solid texture fairly well when the kernels are used in conjunction with the LDA. It is important that a sufficient number of the training data sets is used for the LDA regarding the number of shape features.

| | C | M | T | W |
|---|---|---|---|---|
| C | 25 | 0 | 0 | 0 |
| M | 0 | 16 | 0 | 9 |
| T | 0 | 1 | 24 | 0 |
| W | 0 | 9 | 0 | 16 |

3×3×3

| | C | M | T | W |
|---|---|---|---|---|
| C | 25 | 0 | 0 | 0 |
| M | 0 | 25 | 0 | 0 |
| T | 0 | 0 | 25 | 0 |
| W | 0 | 0 | 0 | 25 |

5×5×5

Fig. 13. A Classification Rate Table (3×3×3 Laws Kernels and 5×5×5 Laws Kernels). The labels 'C', 'M', 'T' and 'W' in the figure indicate types of textures. The 5×5×5 kernels classify 3D solid texture fairly well when the kernels are used in conjunction with the LDA.

## IV. Conclusions

3D solid textures were analyzed by the extended Laws texture energy measure approach. Three dimensionally extended Laws convolution kernels were used for analyzing 3D volumetric data. Experimental 3D solid textures were synthesized by using a simulation software program. A classification efficiency of the extended Laws kernels was evaluated. In our preliminary experimental, 3D solid textures classified fairly well when the 5×5×5 kernels were used in conjunction with the LDA.

In our experiments, only four types of 3D solid textures were used for evaluating the extended Laws convolution kernels. For future experiments, additional solid textures which contain various patterns will be examined. Also, other statistical approaches such as a quadratic discriminant analysis (QDA) will be applied in conjunction with the Laws convolution kernels for improving classification rates.

## Acknowledgements

This research was partially supported by grants from the KAKENHI (YR-21700127, 2009).

## References

[1] R. M. Haralick, K. Shanmugam, I. Dinstein, Textural Features for Image Classification, *IEEE Trans. Sysmtems Man Cybernetics*, Vol.3, No.6, pp.610–621, 1973.

[2] T. Kato, Database architecture for content-based image retrieval, *Proc. SPIE Image Storage Retrieval System*, 1662, pp.112–123,1992.

[3] T. Randen and J.H. Husoy, Filtering for texture classification: a comparative study, *IEEE Transactions on Pattern Analysis and Machine Intelligence*, Vol. 21, Issue 4, pp.291-310, 1999.

[4] R. C. Veltkamp and M. Tanase, Content-Based Image Retrieval Systems: A Survey, Technical Report UU-CS-2000-34,Institute of Information and Computing Science, University Utrecht, 2000.

[5] D. H. Xu, A. Kurani, J. D. Furst, D.S. Raicu, Run-length encoding for volumetric texture, *The 4th IASTED International Conference on Visualization, Imaging, and Image Processing*, 2004.

[6] D. Gao, Volume texture extraction for 3D seismic visualization and interpretation, *Geophysics* vol. 68, issue 4, pp. 1294–1302, 2003.

[7] Mahmoud-Ghoneim D, Toussaint G, Constans JM, de Certaines JD, Three Dimensional Texture Analysis in MRI: a preliminary evaluation in gliomas, *Magnetic Resonance Imaging*, Vol. 21-9, pp.983-987, 2003.

[8] A. Kurani, D. H. Xu, J. D. Furst, D.S. Raicu, Co-occurrence matrices for volumetric data, *The 7th IASTED International Conference on Computer Graphics and Imaging*, 2004.

[9] F. Tsai, C. Chang, J. Rau, T. Lin and G. Liu, 3D Computation of Gray Level Co-occurrence in Hyperspectral Image Cubes, *Lecture Notes in Computer Science: Energy Minimization Methods in Computer Vision and Pattern Recognition*, Vol. 4679, pp.429–440, 2007.

[10] M. T. Suzuki, Y. Yaginuma, and N. Osawa, A HLAC Shape Descriptor Extraction Method for 3D Solid Textures, *The World Scientific Engineering Academy and Society Transaction on Computers*, Issue 3, Vol.3, pp.768-773, ISSN:1109-2750, 2004.

[11] M. T. Suzuki, Y. Yaginuma, A Solid Texture Analysis Based on Three Dimensional Convolution Kernels, *Electronic Imaging 2007, Videometrics IX, (EI-2007), Proc. of SPIE and IST Electronic Imaging*, SPIE Vol. 6491, 64910W pp.1-8, 0277-786X/07/ San Jose, USA, 01/2007.

[12] K. I. Laws, Texture energy measures. *DARPA Image Understanding Workshop*, pp.47–51. DARPA, 1979.

[13] K. I. Laws, Rapid texture identification. *In SPIE Vol. 238 Image Processing for Missile Guidance*, pp.376-380, 1980.

[14] D. S. Ebert, F. K. Musgrave, D. Peachey, K. Perlin, and S. Worley, Texturing and Modeling, A Procedural Approach, ISBN 0-12-228760-6, Academic Press, 1994.

[15] Ken Perlin, An image synthesizer, *Computer Graphics, (SIGGRAPH 1985 Proceedings)*, Vol.19, pp.287296, 1985.

[16] K. S. Fu and S. Y. Lu. Computer generation of texture using a syntactic approach, *Computer Graphics (SIGGRAPH 1978)*, Vol.12, pp.147-152, 1978.

[17] S. Haruyama and B. A. Barsky, Using stochastic modeling for texture generation, *IEEE Computer Graphics and Applications*, 4(3) pp.7-19, 1984.

[18] B. J. Schacter and N. Ahuja, Random Pattern Generation Processes, *Computer Graphics and Image Processing*, Vol.10, pp.95-114, 1979.